Mechanical and Aerospace Engineering
B. Guan (Ed.)

doi:10.3233/ATDE250037

Performance Simulation and Flight Test of the High-Maneuverability Target Drones

Le GAO[1,2,3] , Guangquan LV[1*], Qihang YUAN[1], Ying BI[1], Zijian ZHANG[1]
[1] Institute of Engineering Thermophysics, Chinese Academy of Sciences, Beijing, 100190, China;
[2] School of Aeronautics and Astronautics, University of Chinese Academy of Sciences, Beijing, 100049, China;
[3] National Key Laboratory of Science and Technology on Advanced Light-Duty Gas-Turbine, Beijing, 100049, China;

Abstract. Maneuverability is an important indicator for evaluating the comprehensive performance of aircraft, and the researchers have increasingly high requirements for the maneuverability of fighters. As target simulators, drones must possess corresponding maneuvering capabilities to replicate real combat scenarios. Based on the requirements of modern weapon testing systems and current trends in target drone technology, investigations into the development of supersonic high-maneuverability target drones was considered. Key performance metrics such as aerodynamic characteristics, structural integrity, and flight performance were tested. As a preliminary validation, development and flight testing of high-maneuverability, overload-capable target drones were conducted. For a drone with a total weight of 248 kg and a maximum flight speed of 0.8 Ma, the goal is to achieve a stable overload capability of over 6g and a maximum overload of over 9g. Firstly, CFD and CSD techniques were used to simulate the key performance of the aircraft, then flight tests were conducted for verification. The results indicate that the flight performance meets the overall design requirements and the simulation results agrees with it. The drone achieved complete autonomous control from take off to landing. The entire system performed reliably, and the drone maintained stable flight, with normal attitude, speed, altitude, and flight path tracking.

Keywords Target drone UAV system, high maneuvering overload, first flight test, ground test

1. Introduction

The target drone is a powered, unmanned military aircraft designed to simulate aerial threats. It replicates the motion and detectability of the simulated object, enabling the testing of air weapon systems and training combat units. The primary targets of air defense weapons include fighter jets and cruise missiles, necessitating target drones that closely match the performance of these threat targets. This allows for the simulation of various real-world targets to effectively evaluate air defense weapon performance.

Live-fire testing gained importance after the Vietnam War, where U.S. air-to-air missiles underperformed, achieving less than 40%, sometimes below 20%, of the expected 90% kill rate [1][2]. As a result, the U.S. mandated comprehensive lethality

* Corresponding Author: Guangquan LV, lvguangquan@iet.cn

testing for all major missile projects before production, requiring testing in realistic conditions, including air-to-air and air-to-ground scenarios with full-scale target drones. The concept of unmanned target aircraft began in the 1930s and evolved into key military assets. The U.S. pioneered remote-controlled vehicles, with the first flight in 1909. By 1937, remote-controlled aircraft were explored as targets, leading to the MQM-33/36 flight in 1945[3][4]. The BQM-34 and BQM-74 Chukar are notable subsonic targets, while supersonic targets like GQM-163 "Coyote" and AQM-81 "Firebolt" simulate advanced missile threats. The U.S. also developed full-size targets, such as the QF-4 and QF-16, and the 5GAT to replicate stealth aircraft. This led to a complete system of target drones covering all speeds, altitudes, and stealth capabilities[5-11].

China has over fifty years of target drone development, establishing a comprehensive system from low-speed to supersonic, and low-altitude to high-altitude, including non-stealth and stealth targets. Notable models include Type II-150, Sky Eagle, and the II-300J UAV. The II-300J, presented in 2020, supports multi-aircraft coordination, simulating complex scenarios with interference and electronic countermeasures, closely replicating combat environments. China continues developing subsonic and supersonic high-maneuver stealth target drones[12][13].

As a critical component of weapon system testing, target drones have seen rapid development under increasing global emphasis. The level of a country's target drone technology indirectly reflects the overall performance of its air defense systems. The realism with which a target drone simulates threat targets fundamentally determines the operational effectiveness of air defense equipment[14]. While nations are accelerating the development of new aerial combat systems, target drone development also aims to accurately simulate the characteristics of next-generation air combat platforms. The main potential development directions are as follows:

(1) Current stealth target drones mainly focus on forward-facing stealth but lack sufficient side and rear stealth, limiting the accuracy of their radar cross-section (RCS) distribution. A new generation of target drones should adopt a flying wing layout, similar to the NGAD concept, to improve all-directional stealth[15].

(2) While the target drone does not need sustained supersonic cruise, supersonic flight is crucial. Supersonic speeds influence fuse activation, target damage effectiveness, and radar tracking accuracy, making supersonic flight and maneuvering essential capabilities for next-generation target drones.

(3) High maneuverability is key to replicating modern combat scenarios. Sixth-generation manned aircraft will surpass fifth-generation fighters in maneuverability, with unmanned systems likely to exceed these levels due to the absence of pilot constraints. Target drones must match these capabilities to effectively simulate combat scenarios.

Research into supersonic, high-maneuverability target drones is underway, focusing on critical technology validation and platform development. Initial tests have evaluated key performance aspects such as aerodynamics, stability, and structural integrity, laying the foundation for future development. The first flight test has been completed, providing valuable data for ongoing research

In the present work, the first flight test of the target aircraft system is described in detail in four parts. Section 2 provides a detailed overview of the target drone system. Section 3 introduces the main content of the flight test and offers a comprehensive analysis of the data obtained from the flight test. Finally, Section 4 presents the comments and conclusions.

2 The Target Drone UAV System

2.1. Subsystem of Aircraft

2.1.1 Structure Design

The high-maneuverability target drone discussed in this paper employs a conventional design with a trapezoidal wing of medium aspect ratio, underwing side air intakes, a single vertical tail, and fully movable horizontal stabilizers in a standard configuration. The design features large strakes and a blended wing-body structure. The wings have a medium aspect ratio with small leading-edge radii and low camber airfoils, while the tail uses thin symmetric airfoils. The wings do not have ailerons; aileron functionality is achieved through differential movement of the all-moving horizontal stabilizers. The high-maneuverability target drone's fuselage houses a turbojet engine, rudder servos, and tail control actuators. The mid-fuselage contains the air intake, countermeasure dispensers, and fuel system. The forward section primarily accommodates flight control equipment, electrical systems, data link devices, payloads, and a recovery parachute. Figure 1 illustrates the overall layout.

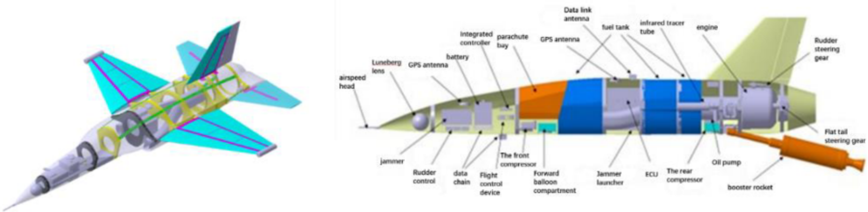

(a) The target drone Structure Component Diagram (b) The target drone General Arrangement

Figure 1. The overall layout of the target machine

Table 1. The target drone Outline Parameters.

Items	Parameter
Overall Length /m	3.548
Overall Height /m	0.904
Wingspan /m	2.596
Wing Area /m^2	1.837
Average Chord Length of Wing /m	0.8
Wing Aspect Ratio	3.67
Flat Tail area /m^2	2×0.198

2.1.2 Aerodynamic Characteristics

To avoid strong disturbances from the intake and blunt aft body affecting the flow field and aerodynamic coefficient calculations, a non-powered ventilation approach is used. The intake boundary is placed slightly inside, with static pressure set at 95% of the free-stream value, simulating natural ventilation. At the exhaust nozzle, the exit boundary matches free-stream temperature and pressure, serving only to prevent flow separation at the blunt aft body without adding extra energy.

Figure 2 illustrates the longitudinal aerodynamic characteristics. The lift coefficient increases with the angle of attack for all Mach numbers, showing good lift generation capabilities. The slope of the lift curve remains relatively consistent, indicating minimal Mach effect on lift. The drag coefficient rises significantly with increased attack angles and is higher at greater Mach numbers, typical of aerodynamic behavior. The moment coefficient becomes more negative with increased angle of attack, suggesting stable characteristics. The lift-to-drag ratio peaks around an attack angle of 4° to 6°, with efficiency decreasing sharply beyond this point. The aircraft demonstrates favorable longitudinal characteristics: stable lift generation, predictable drag, and a stable moment profile. The optimal range for efficient flight lies at an attack angle of 4° to 6°, balancing lift and drag, with stable flight behavior across varying speeds.

For all Mach numbers, the side force coefficient decreases linearly with increasing sideslip angle, becoming more pronounced at higher angles of attack, indicating increased sensitivity. The yawing moment coefficient also increases linearly with sideslip angle, suggesting a restoring yawing moment favorable for stability. These characteristics remain consistent across different attack angles, showing stable yawing behavior. Overall, the aircraft demonstrates strong lateral-directional characteristics, with linear side force and yawing moment behavior, ensuring predictable responses and stable directional control across different flight conditions.

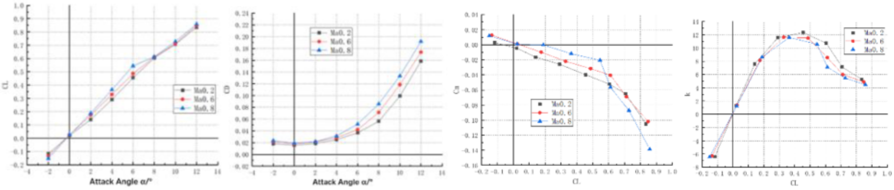

Figure 2. Longitudinal aerodynamic characteristic

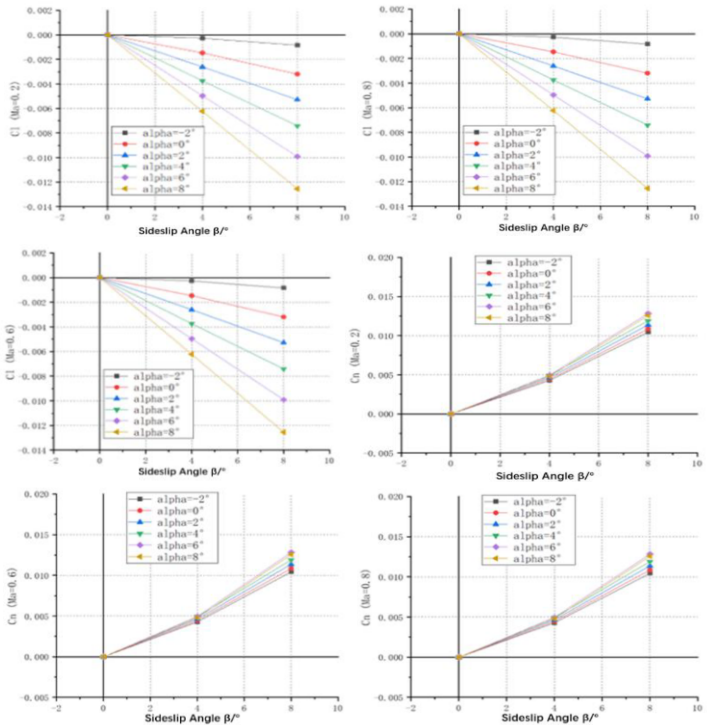

Figure 3. Lateral aerodynamic characteristic

2.1.3 Strength characteristics

To analyze the load conditions of the target aircraft, the most severe scenarios on the ground and during flight were selected, including takeoff, high-maneuverability flight, and parachute recovery conditions.

Static strength simulation analysis under high-maneuverability flight conditions indicates that the maximum displacement under ultimate load is approximately 52.9 mm, and the wingtip twist angle is about 0.39°. The stress and strain in all parts remain within the allowable limits of the material. The displacement and strain contours are shown in Figure 4.

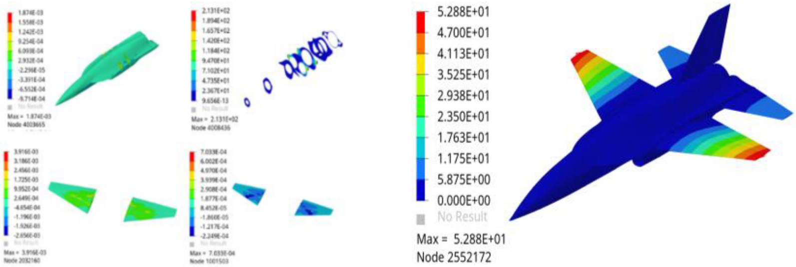

(a) Displacement deformation under ultimate load (b) Strain of each component under ultimate load

Figure 4. Contours of high maneuvering flight conditions

2.2. Flight Control Avionics System

The flight control system of the target drone, shown in Figure 5, includes a flight control computer, MEMS inertial guidance, and a servo system. The drone's mission modes consist of standby, test (stabilization, hand control, frequency sweep), and work (take-off, mission flight, hover, landing). Longitudinal flight modes include level flight, fixed height/speed, climbing, etc., while transverse modes include trajectory tracking and maneuvers. Flight mode transitions can occur autonomously, following pre-programmed plans, or via remote control from a ground station, offering flexibility for different missions.

The flight control system manages stable flight using guidance and control laws, generating commands for rudder surfaces and engine speed. Outer-loop guidance law corrects longitudinal deviations, while inner-loop control manages challenges like aerodynamic nonlinearity and mass center shifts during maneuvering. To address these challenges, the system uses modern control methods like Active Disturbance Rejection Control (ADRC) in addition to traditional PID. The LESO-based technique enhances disturbance rejection and dynamic performance, significantly improving control quality and stability across different flight conditions.

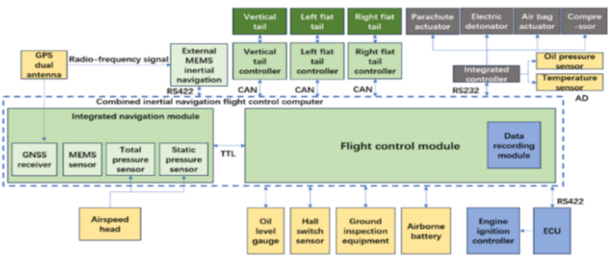

Figure 5. Interconnection diagram of flight control system related equipment

3. Autonomous Flight Test

3.1. Main Contents of Flight Test

The target drone conducted flight tests included: (1) rocket assisted takeoff; (2) Wait for the watch speed to climb quickly; (3) Low altitude cruising; (4) Limit up and instruction testing; (5) Hollow cruising; (6) Slow down and slide down; (7) Open the umbrella for recycling. The launch process of the UAV was smooth, the attitude was stable during the flight, the track tracking and speed control were accurate, the engine successfully completed the high-altitude cruise process. It took 1 minute from parachute deployment to ground contact recovery. During the flight test, the drone autonomously flew for 34.6 minutes, with a range of 340 km, a maximum Mach number of 0.63, a maximum true airspeed of 194 m/s, a maximum climb rate of 38 m/s, and a maximum altitude of 8032 m.

The main purpose of the first flight test of the target drone prototype is to verify the functions of various subsystems (aircraft, power system, fuel system, navigation and control system, avionics system, data link system and launch and recovery system, etc.). It obtained flight test data, validated the flight control law, verified the flight control law, mastered the stability characteristics and flight performance of the aircraft, tested the adaptability of the system hardware to the mid-air flight environment.

3.2. Launch Stage Analysis

The target drone was launched due west on a preset course with an initial launch Angle of 13.8° and an initial roll Angle of 0.8°. The booster worked for about 2s, and it separated smoothly after the end of the work. As shown in Figure 6(a), the maximum pitch Angle is 18.8°, and the maximum left roll of the UAV is 5.6°. Flight control began to control the attitude of the UAV after 0.7s of launch, and the attitude was normal during launch. Its rudder deviation is shown in Figure 6(c). The rudder deviation command logic is consistent with the UAV attitude condition, the rudder output follows the command, and the rudder surface deflection is normal during launching. The flight speed change in the launch stage was shown in Figure 6(e), and the indicated speed at the end of the launch reached 84.7m/s. The GPS altitude change is shown in the following figure, and the final launch climb is about 26m. The overload situation of the UAV in the launch stage is shown in Figure 6(f). The working time of the rocket booster is about 2s, the maximum axial overload is close to 5.72g, the normal overload is about 1.7g, the lateral overload is close to 0. The target drone demonstrated stable performance during the launch phase, with the booster successfully separating and the flight control system effectively managing the attitude. Parameters such as speed, altitude gain, and overload were all within normal ranges, confirming the reliability and stability of the system design.

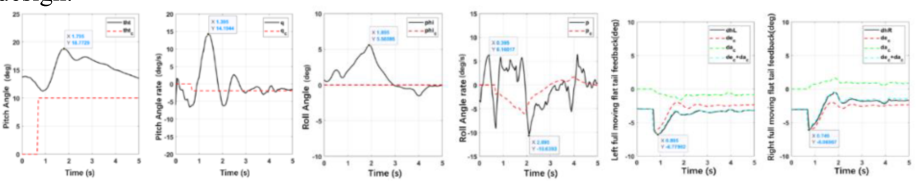

(a) Pitch angle and pitch angle rate **(b) Roll angle and roll angle rate** **(c) Full motion flat tail deflection**

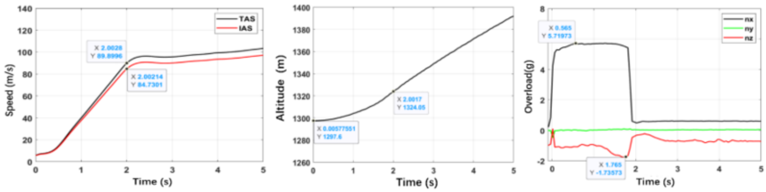

(d) Emission velocity (e)Elevation variation (f) Emission overload

Figure 6. Changes in physical quantities over time during the launch phase

3.2.1 Analysis of aerodynamic characteristics of the launch stage

The pitch Angle of the launch section of the target drone is shown in Figure 7. The simulation was conducted using a thrust line 2mm below the center of mass, and compared with the flight test, the simulation model showed lower rotational inertia and damping. The reasons for the deviation include: the magnitude of the thrust of the main engine, the position of the center of mass of the booster and the changes in the center of mass during the consumption of the propellant, the aerodynamic characteristics of the pitch moment of the booster during operation, ground effects, the actual thrust of the rocket booster, and the rotational inertia of the combination. After 7 seconds, the pitch Angle can track the 10 degree pitch command.

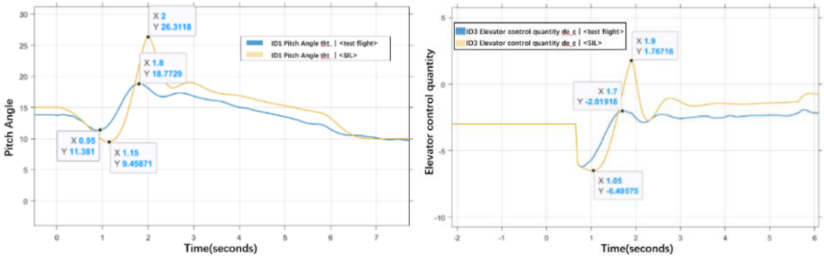

Figure 7. Pitch Angle and elevator of launch stage

The final velocity and altitude of the boost stage are illustrated in Figure 8. The SIL simulation predicts a boost duration of 1.87 seconds, whereas the flight test recorded a boost duration of 2.17 seconds, with both scenarios achieving a final velocity of 90 m/s. Due to variations in pitch angle in the SIL model during the boost stage, the simulated boost altitude is 22 meters, which is 30 meters lower than that in the flight.

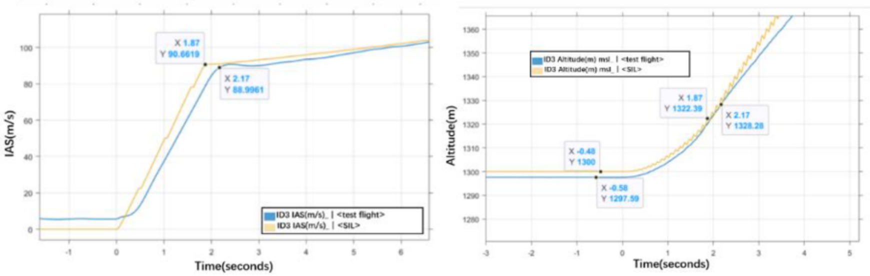

Figure 8. Altitude and indicated speed of launch stage

3.2.2 Flight control system analysis of launch stage

The flight parameters of the target drone during launch were shown in Figure 9. It can be seen that the maximum rolling Angle phi = 5.6°, the maximum pitch Angle tht = 18.8°, the maximum flat-tail rudder deviation dh = −6.8°, and the rudder deviation dr = −1.2° during launch.

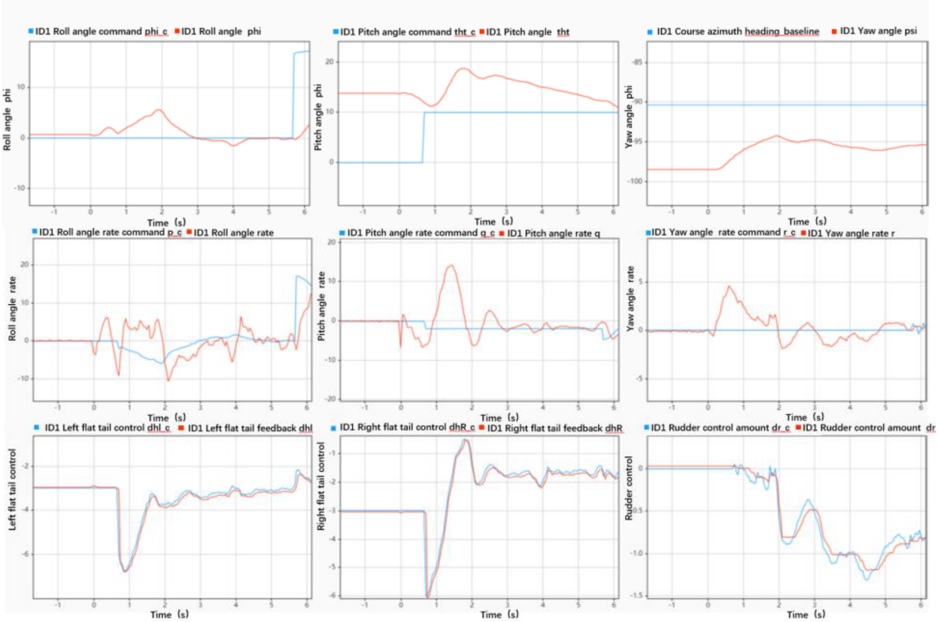

Figure 9. Launch stage data

3.3. Level Flight Stage Analysis

3.3.1 Analysis of aerodynamic characteristics of level flight stage

This work compares the SIL simulation results with flight data for the analysis of the 5000 meter altitude ascent phase. In the flight, the throttle setting was 0.82 (385 N), which is 32 N higher than the SIL simulation value of 0.81 (353 N). This suggests that the flight drag is approximately 10% greater than that predicted by the simulation model. The equivalent drag coefficient difference is calculated as ΔCD=0.0018. In SIL simulation, the clearance in the elevator system is 0.3 degrees, while in flight it is 0.1 degrees and it in the rudder system is 0.5 degrees, while in flight it is 0.4 degrees.

The aerodynamic characteristic analysis indicated that at an altitude of 5000 meters, the combined error between the aerodynamic and engine models was less than 5%. At an altitude of 8000 meters, this error increased to less than 10%. Furthermore, the SIL simulation showed that the gaps in both the elevator and rudder systems were slightly larger than those observed in flight.

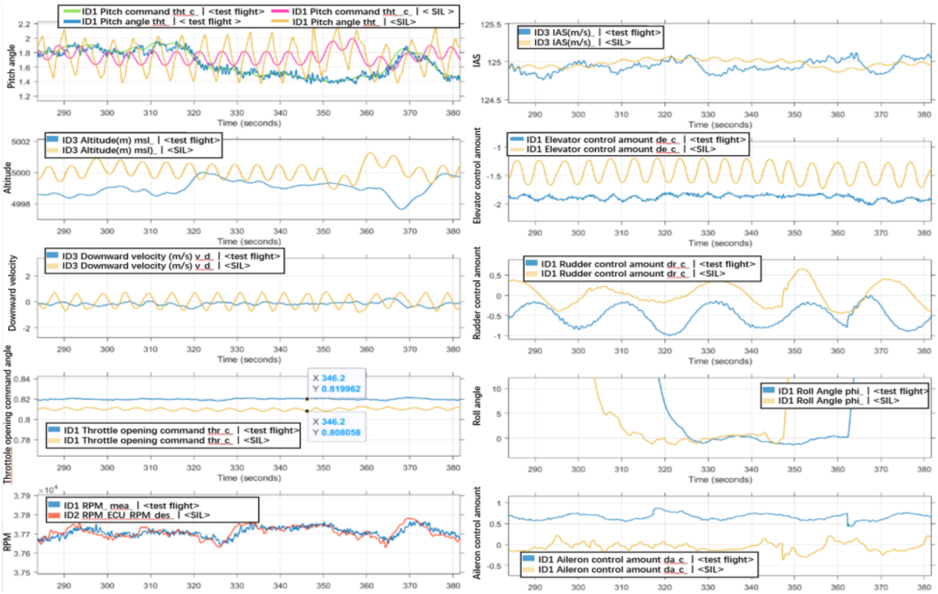

Figure 10. Main parameters of level flight stage

3.3.2 Flight control system analysis of level flight stage

Based on the flight data, the variation of key parameters for the target drone during a typical level flight stage are illustrated in Figure 11. It is evident that under stable level flight conditions, the UAV's pitch angle amplitude is ≤1.5°, and the roll angle amplitude is ≤1.5°, which demonstrates the reasonableness of the control laws. Additionally, during stable level flight, the UAV's indicated airspeed deviation is ≤0.25 m/s, the lateral position offset is ≤13 m, and the altitude deviation is ≤2 m, indicating that the performance of the aircraft aligns with the design specifications. Furthermore, the presence of steady-state trim values in the ailerons and rudder during the flight test may be attributed to factors such as static errors in the inertial navigation system's horizontal plane, aerodynamic asymmetry, lateral center of gravity deviations, or thrust line misalignment.

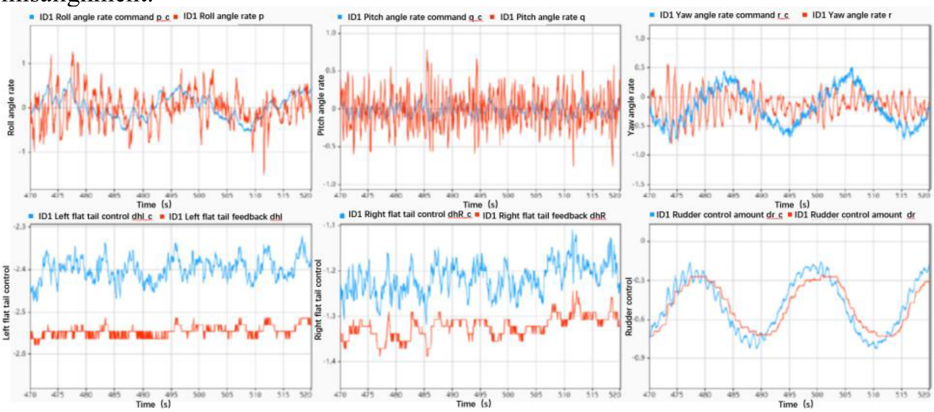

Figure 11. Flight data of typical level flight stage

4. Conclusion

Based on the requirements of modern weapon testing systems and the development trends of target drone technology, this paper conducts an in-depth study of a high-maneuverability target drone. Firstly, computational fluid dynamics (CFD) and computational structural dynamics (CSD) techniques were utilized to comprehensively test and analyze key performance indicators, such as the aerodynamic characteristics, structural integrity, and flight performance of the target drone. The simulation results demonstrate that the overall technical design of the target drone is reasonable and reliable, with all technical specifications meeting the design requirements.

Subsequently, flight tests were conducted to validate the target drone. The test results showed that the target drone achieved a maximum flight speed of 0.63 Mach and demonstrated stable overload capability of up to 6g. Moreover, fully autonomous control was realized throughout the entire flight process, from takeoff to landing. During flight, the UAV maintained stable conditions, exhibiting normal attitude, speed, altitude, and trajectory tracking. Overall, the results indicate that the flight performance of the target drone fully meets the overall design requirements, and the entire system operates reliably, showcasing its potential for application.

References

[1]. Carter D, Burris P, Brandt S. Fifth-Generation target drone project initial development[R]. *AIAA* 2011-**7011**, 2011.

[2]. Fangfang Yan, Guanzhang Yuan, Kexu Deng. Study on the present situation and key technology and development trend of target technology[C]//*The 9th Yangtze River Delta Science and Technology Forum-Proceedings of Aerospace Science and Technology Innovation and Yangtze River Delta Economic Transition. Nanjing: Jiangsu Institute of Aeronautics and Astronautics*,2012: **10**.

[3]. Songhai Fu, Mingqing He, Baolin Wu, Suzhong Zhang. The development trend of the target system[C]//*Proceedings of the 5th China UAV Conference*. Beijing: Aviation Industry Press, 2014: **28**-30.

[4]. Report of the Defense Science Board Task Force on Aerial Targets[R]. *Office of the Under Secretary of Defense for Acquisition, Technology and Logistics*. Washington，D. C.，October 2005.

[5]. Delaney W P, Williams M. Report of the Defense Science Board Task Force on Aerial Targets[J]. *Report of the defense science board task force on aerial targets*, 2005.

[6]. Daobo W, Jingguang R, Wanyue J, et al. *An overview of the development of target drones and associated autonomous control[J]. Science & Technology Review*, 2017.

[7]. Wei D, Yuan O U, Gen-Zhu S, et al. *Research on aerial target development of U.S. Navy[J]. Ship Science and Technology*, 2018.

[8]. Carter D, Burris P, Brandt S. Fifth-Generation target drone phase I design[R]. *AIAA* 2011-**7012**, 2011.

[9]. Brandt S, Carter D, Burris P. Fifth-Generation target drone phase II[R]. *AIAA* 2011-**7013**， 2011.

[10]. Burris P, Carter D, Brandt S. Fifth-Generation target drone phase III design[R]. *AIAA* 2011-**7014**, 2011.

[11]. Kepeng Liu,Shishan Wang, Bowen Fang. Development History and Current Trends of Target Aircraft.[C]//*Proceedings of the 2022 Annual Meeting of the China Aviation Industry Technology and Equipment Engineering Association*..2022.**055241**.

[12]. Wei Ding, Yuan Ou, Genzhu Shi, etc. Study on the Development of 5GAT[J]. *Ship Science and Technology*, 2018, **40** (21): 170-173

[13]. Daquan Du, Guiyang Hu, Da Meng. Research on the Development of New Generation Target Drone System[J]. *Aero Weaponry*,2023, **(6)** : 27－31 .

[14]. Beheshtipour Z, Khaloozadeh H. An innovative fuzzy covariance presetting for high maneuvering target tracking problems[C]//*2009 Chinese Control and Decision Conference. IEEE*, 2009: **5623-5628**.

[15]. Rahnama S, Arvan M R. Comparison of extended and unscented Kalman smoother in deriving kinematic characteristics of a high maneuver flying target[C]//*Proceedings of 2011 International Conference on Modelling, Identification and Control. IEEE*, 2011: **537-542**.